

UC Riverside

UC Riverside Previously Published Works

Title

Improving the estimation of evaporation by the FAO-56 dual crop coefficient approach under subsurface drip irrigation

Permalink

<https://escholarship.org/uc/item/9bm510m3>

Journal

Agricultural Water Management, 178(C)

ISSN

0378-3774

Authors

Phogat, V
Šimůnek, J
Skewes, MA
et al.

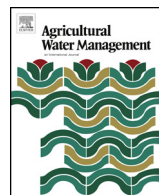
Publication Date

2016-12-01

DOI

10.1016/j.agwat.2016.09.022

Peer reviewed



Improving the estimation of evaporation by the FAO-56 dual crop coefficient approach under subsurface drip irrigation



V. Phogat^{a,*}, J. Šimůnek^b, M.A. Skewes^a, J.W. Cox^{a,c}, M.G. McCarthy^a

^a South Australian Research and Development Institute, GPO Box 397, Adelaide, SA 5001, Australia

^b Department of Environmental Sciences, University of California, Riverside, CA 92521, United States

^c The University of Adelaide, PMB1, Glen Osmond, SA 5064, Australia

ARTICLE INFO

Article history:

Received 8 July 2015

Received in revised form

13 September 2016

Accepted 24 September 2016

Keywords:

FAO-56 dual crop coefficient

Evaporation

Subsurface drip

Evapotranspiration

Wine grape

ABSTRACT

Partitioning of evapotranspiration and estimating of irrigation contribution to evaporation play a crucial role in managing scarce water resources and help in increasing the water productivity of crops, especially of sparsely vegetated plants. In this study, the FAO-56 dual crop coefficient (DCC) approach for estimating evaporation from soil under cropped conditions is adapted for subsurface drip irrigation (SDI). This new approach involves one additional variable, the fraction of the irrigation depth contributing to evaporation ($f_{I,Es}$), which was defined and integrated into the FAO-56 equations for estimating daily water balance from the evaporation layer (0–15 cm). Impacts of soil texture, heterogeneity, irrigation depth, design parameters of the irrigation system on $f_{I,Es}$, and the fraction of the soil surface wetted by irrigation (f_w) (and consequently the exposed and wetted fraction (f_{ew})), were evaluated through HYDRUS-2D simulations. The modified procedure was compared with the existing FAO-56 method for estimating components of annual ET for wine grape under SDI.

The model simulations showed that the $f_{I,Es}$ fraction in a homogeneous, isotropic light-textured soil was minimal (0.04) when SDI was placed at a depth of 25 cm. However, in medium and heavy textured soils $f_{I,Es}$ was 4 times larger than in light-textured soils. The value of f_w was slightly higher in fine-textured (0.09) than in medium-textured soils (0.07). In Duplex soils with two contrasting textural layers, f_w (0.12–0.16) was higher due to the presence of a heavy-textured soil layer just below the drip line. Similarly, in Triplex soils (3 different textural layers), placing the drip line in the middle layer effectively reduced both $f_{I,Es}$ and f_w close to zero. In contrast, f_w (0.18–0.30) and $f_{I,Es}$ (0.28–0.42) both increased considerably in heterogeneous soils. Both fractions (f_w and $f_{I,Es}$) increased with an increase in irrigation depths, except for $f_{I,Es}$ in loamy sand. The fractions were slightly lower when a drip line was placed at a depth of 10 cm (an evaporation zone) than when it was placed on the soil surface. Applying the same amount of water with different discharge rates had little impact on $f_{I,Es}$ and f_w fractions. An increase in the drip line spacing proportionally decreased the wetted fraction on the soil surface. Annual evaporation for SDI irrigated wine grapes at the field study site, estimated using the existing FAO-56 procedure, was overestimated by about 5–6% compared to using the modified procedure. However, this deviation between the two approaches increased (18%) for heavier soil textures. It is concluded that the existing FAO-56 procedure needs to be adjusted when used to estimate evaporation under subsurface drip irrigation. However, the impact of the proposed modification on evaporation needs further evaluation under other crops, soils, and climatic conditions.

© 2016 Elsevier B.V. All rights reserved.

1. Introduction

Partitioning of ET into evaporation (E_s) and transpiration (T_p) is important for proper scheduling of irrigation for crops, espe-

cially under drip irrigation systems where partial wetting of the soil surface and high system design costs increase the importance of optimal management of the system. While E_s is considered to be an undesirable water loss, T_p is assumed to be an essential component of crop water productivity. There can be huge losses of water through evaporation, particularly in sparsely planted trees and orchards, such as grapevines, where a large soil surface area is exposed to atmospheric effects. For example, the E_s/ET ratio was

* Corresponding author.

E-mail addresses: vinod.phogat@sa.gov.au, vinphogat@gmail.com (V. Phogat).

found to exceed 30% in 32 out of 52 ET partitioning studies (Kool et al., 2014a). Hence, reliable estimation of E_s can help in managing the unproductive losses of irrigation water because it provides useful information for irrigation management and water use efficiency improvements.

The FAO-56 dual crop coefficients (DCC) approach (Allen et al., 1998) is accepted as a standard technique in the absence of measured data to calculate crop evapotranspiration demand and to estimate E_s losses, using a basal crop coefficient (K_{cb}) and an evaporation coefficient (K_e). This technique is also employed to estimate potential T_p and E_s in agro-hydrological modelling studies (Ramos et al., 2012; Kool et al., 2014b; Phogat et al., 2013, 2014). The reference ET (ET_0) is calculated using a modified Penman-Monteith equation, which incorporates a number of weather and energy balance parameters, as described in Allen et al. (1998). Other improvements in estimating crop evapotranspiration (ET_C) are explained in subsequent publications (Allen et al., 2005a,b; Allen and Pereira, 2009).

Surface drip (DI) and subsurface drip (SDI) irrigation are relatively recent methods of water application in irrigated agriculture. The procedure for estimating E_s and T_p by the FAO-56 DCC approach works well for surface drip, where water is applied on the soil surface from where it spreads radially while infiltrating down into the soil, in a process similar to that under sprinkler irrigation. Subsurface drip, however, applies water below the soil surface, from where water moves in all directions (including upwards) depending on the soil hydraulic properties and moisture regime. The FAO-56 DCC approach calculates E_s from the evaporation zone, which in many cases is located within the top 0.10 to 0.15 m soil layer (Allen et al., 1998). Given that emitters in an SDI system may be installed below the evaporation zone, it is clear that the fraction of applied irrigation, which moves through the evaporation zone ($f_{l,Es}$), and is therefore available to contribute towards E_s , is potentially much smaller under SDI than under DI or sprinkler irrigation. Consequently, estimates of variables used in the FAO-56 procedure, such as the fraction of the wetted soil surface (f_w), the fraction of the soil surface wetted and exposed to evaporation (f_{ew}), the irrigation depth for the fraction of the wetted soil surface (I_w) and the irrigation depth that infiltrates into the soil (I_i), will be different between SDI and DI. For example, Cancela et al. (2015) reported f_w values to be 10 times higher for DI (0.1) than for SDI (0.01). These parameters have a significant impact on the estimation of evaporation for subsurface drip irrigation. Hence, there is need to modify the current estimation procedure for the soil evaporation coefficient (K_e) for SDI systems.

While the entire SDI system could be evaluated using process-based numerical models, rather than the simplified FAO-56 DCC approach, such models are relatively difficult to use and parameterize, and thus unlikely to be adopted by farmers. On the other hand, the FAO-56 empirical approach Allen et al. (1998) is much simpler, providing that its empirical parameters can be estimated, and more widely used for practical applications. One of the objectives of this manuscript thus is to modify the existing FAO-56 approach so that it is applicable also for the SDI systems and show how additional required parameters can be estimated.

The parameters of the FAO-56 approach are usually obtained based on field experiments. However, field measurements of many of these parameters, such as $f_{l,Es}$ for different irrigation system configurations and for different soils would be a complex and near impossible exercise. On the other hand, there is no fundamental reason, why these coefficients could not be estimated, as an alternative to experimental data, using a process based model that has been widely accepted and validated for describing particular processes involving these parameters. The f_w , f_{ew} and $f_{l,Es}$ parameters can thus be alternatively estimated with the help of numerical models.

Among available numerical models, HYDRUS-2D (Šimůnek et al., 2008) has been extensively used in evaluating the impact of various irrigation system designs (e.g. Skaggs et al., 2010; Phogat et al., 2012; Naglic et al., 2014) and in solving other water balance and solute transport problems for surface (e.g. Phogat et al., 2013, 2014; Elmalioglu et al., 2013; Li et al., 2015) and subsurface (e.g. Cote et al., 2003; Lazarovitch et al., 2005; Singh et al., 2006; Kandelous et al., 2012; El-Nesr et al., 2014) drip systems. Provenzano (2007) and Kandelous and Šimůnek (2010) tested this model for modelling water distribution around the subsurface dripper with variable drip line placements and drip discharges, and compared the dimensions of the wetted zone in laboratory and field conditions involving soils of varied textures. Similarly, Skaggs et al. (2004) showed that HYDRUS-2D simulations matched well a uniform wetted pattern along a SDI drip line with a dripper distance of 30 cm in the field. According to the ISI's Web of Science (Šimůnek et al., 2016), HYDRUS-2D model has been successfully used to simulate drip/trickle irrigation in more than 80 peer-reviewed journal manuscripts. It is thus very likely that a calibrated HYDRUS model can provide reliable results as a surrogate to field experimental data. Therefore, HYDRUS-2D can be employed to estimate $f_{l,Es}$ and f_w for different soil textures, soil horizon heterogeneity, and for different irrigation system designs.

The objectives of this investigation were (a) to compute the potential fraction of the irrigation depth entering the evaporation zone ($f_{l,Es}$) and wetted soil surface fraction (f_w) (and from this the exposed and wetted fraction, f_{ew}) for field soil using HYDRUS-2D, (b) to simulate the impact of soil type, soil heterogeneities, and drip designs on f_w and $f_{l,Es}$ for SDI in hypothetical scenarios, and (c) to compare the seasonal ET components (T_p , E_s and ET_C) of the wine grapes estimated by the original and the modified FAO-56 DCC approaches for two seasons (2010–11 and 2011–12) for field conditions and for other hypothetical uniform soils. The modified FAO-56 DCC approach incorporates $f_{l,Es}$ fraction in the existing FAO-56 procedure for the estimation of evaporation component for SDI conditions. This modification in FAO-56 DCC is discussed in more details in the following sections.

The field estimated values of daily transpiration (T_p) and evaporation (E_s) by modified FAO-56 approach were used as inputs to HYDRUS-2D in a companion paper (Phogat et al., 2016, under review) which describes the calibration and validation of HYDRUS-2D and the estimation of actual ET components under field conditions for SDI-irrigated wine grapes. The improved FAO-56 procedure could be helpful in providing better estimates of evaporation losses, and could result in improved irrigation scheduling, irrigation efficiency, and water productivity under SDI systems.

2. Materials and methods

2.1. FAO 56: background

The FAO 56 DCC procedure (Allen et al., 1998) utilizes weather data to estimate ET for a reference crop (ET_0) and then multiplies this estimate by a crop coefficient (K_c), which adjusts ET_0 for a specific crop. The reference crop generally represents a clipped, well-watered grass. The potential crop ET (ET_C) may differ from the reference ET (ET_0) as the ground cover, canopy properties, and aerodynamic resistance of a particular crop are different from the reference crop. This procedure has two approaches: i) the single K_c approach, which integrates differences in evaporation and transpiration between field crops and the reference crop into a single crop coefficient (K_c); ii) the dual crop coefficient approach, which separates the crop coefficient into two coefficients: a basal crop coefficient (K_{cb}) responsible for transpiration, and a soil evapora-

tion coefficient (K_e), i.e., $K_c = K_{cb} + K_e$. The equations for estimating ET_C under both approaches are:

$$ET_C = K_{c*} ET_0 \quad (1)$$

$$ET_C = (K_{cb} + K_e)_* ET_0 \quad (2)$$

The calculation of ET_C using these two approaches has been standardized by Allen et al. (1998) and discussed at length by these authors (Allen et al., 2005a,b; Allen and Pereira, 2009). Only the pertinent equations for the dual crop coefficient approach and the modification thereof are described here.

The evaporation coefficient (K_e) expresses the evaporation component of ET_C . It attains a maximum value immediately following precipitation or full cover irrigation, e.g., sprinkler irrigation, and becomes minimal or zero when the soil surface is dry. However, the crop coefficient ($K_c = K_{cb} + K_e$) never exceeds a maximum value (K_{cmax}), which is estimated from the relative humidity, wind speed and crop height as:

$$K_{cmax} = \max \left(\left\{ 1.2 + [0.04(u_2 - 2) - 0.004(RH_{min} - 45)] \left(\frac{ht}{3} \right)^{0.3} \right\}, \{K_{cb} + 0.05\} \right) \quad (3)$$

where RH_{min} represents the mean values of daily minimum relative humidity during the mid- or late season growth stage (%), u_2 is the mean value of daily wind speed at 2 m height during the mid- or late season growth stage (m/s) and ht is the mean plant height during the mid- or late season stage (m). K_{cmax} represents an upper limit on evaporation and transpiration from the cropped surface, and reflects natural constraints on available energy. It ranges from about 1.05 to 1.3 when using the grass reference ET_0 (Allen et al., 2005a).

However, most of the time the evaporation component of K_c (K_e) is reduced below its potential level due to the reduced availability of water for evaporation from the soil. Under these conditions K_e is estimated as:

$$K_e = K_r (K_{cmax} - K_{cb}) \leq f_{ew} K_{cmax} \quad (4)$$

where K_r is the soil evaporation reduction coefficient and its value ranges from 0 to 1 and f_{ew} is the exposed and wetted soil fraction (0.01–1).

When the soil surface is very wet, as happens during precipitation events, $K_r = 1$ (stage 1 evaporation; Ritchie, 1972). However, a few days after a precipitation event, evaporation is reduced below its potential rate ($K_{cmax} - K_{cb}$) and K_r is less than 1, which represents stage 2 of evaporation (Ritchie, 1972). During stage 2 evaporation, K_r is evaluated as:

$$K_r = \frac{TEW - D_{e,i-1}}{TEW - REW} \quad 0 \leq D_{e,i-1} \leq TEW \quad (5)$$

where TEW is total evaporable water (mm) and REW represents readily evaporable water (mm). $D_{e,i-1}$ in Eq. (5) is the cumulative depth of evaporation from the soil surface layer at the end of day $i-1$ (mm), which is estimated by a daily water balance described in Allen et al. (1998), and reproduced as Eq. (7) below. The TEW is estimated as:

$$TEW = 1000 (\theta_{fc} - 0.5\theta_{wp}) Z_e \quad (6)$$

where θ_{fc} is the water content at field capacity (mm), θ_{wp} represents the water content at a wilting point (mm) and Z_e is the evaporating depth (m), or the soil depth from which evaporation draws water, taken as 0.15 m. This is the upper limit of Z_e reported in Allen et al. (1998). The evaporating depth is reported to vary with the texture of the soil, being smaller (0.1 m) in coarse soils and larger (0.15 m) in heavy textured soils Allen et al. (1998). However,

there are contrasting reports in the literature about Z_e for different soils, especially for stage 2 evaporation (Ritchie, 1972). Chanzy and Bruckler (1993) considered Z_e equal to 0.05 m for evaporation measurement from loam, silt clay loam and clay soils. Further complicating the issue, Burt et al. (2005) reported that the K_r values obtained by FAO-56 with $Z_e = 0.1$ m were similar to those measured by Chanzy and Bruckler (1993). Allen et al. (2005b) used a Z_e of 0.15 m for sand, attempting to account for deeper drying depths in the relatively hot climate of Imperial Valley. Torres and Calera (2010) observed that soil evaporation continues even below the 0.15 m soil depth and reported the maximum evaporation depth to be 0.2 m for sandy loam to loam soils. Hence, there is no clear understanding in the literature about the maximum depth of soil contributing to evaporation. Since, we deal with a range of soils and heterogeneity conditions in this study, we use a common value of 0.15 m to have a fixed volume of soil for all scenarios. The daily water balance in the top soil layer is estimated according to Allen et al. (1998, Eq. 77), as:

$$D_{e,i} = D_{e,i-1} - (P_i - RO_i) - \frac{I_i}{f_w} + \frac{E_i}{f_{ew}} + T_{ew,i} + DP_{e,i} \quad (7)$$

where $D_{e,i-1}$ is the cumulative depth of evaporation following complete wetting from the exposed and wetted fraction of the topsoil at the end of day $i-1$ (mm), $D_{e,i}$ is the cumulative depth of evaporation (depletion) following complete wetting at the end of day i (mm), P_i is precipitation on day i (mm), RO_i represents precipitation runoff from the soil surface on day i (mm), which depends on soil surface conditions and intensity and amount of precipitation. However, for relatively flat land and sandy soils RO can be assumed to be negligible (Allen et al., 1998), and this is confirmed by observations at the field site. I_i is the irrigation depth that infiltrates into the soil on day i (mm), E_i represents evaporation on day i (i.e., $E_i = K_e ET_0$) (mm), $T_{ew,i}$ is the depth of transpiration from the exposed and wetted fraction of the soil surface layer on day i (mm), which is assumed to be negligible for deep rooted crops (Allen et al., 1998; Allen, 2000), $DP_{e,i}$ is the deep percolation loss from the topsoil layer on day i when the soil water content exceeds field capacity (mm).

The variable f_w represents the fraction of the soil surface wetted by irrigation (0.01–1) and the variable f_{ew} is the exposed and wetted soil fraction (0.01–1), derived directly from f_w and crop cover (f_c). Drip irrigation applies water to only a small fraction of the soil surface, hence the calculation of evaporation coefficient (K_e) for drip irrigation (both surface and subsurface) requires calculation of the daily water balance for the fraction of the soil surface, which is both wetted and exposed to sunlight (f_{ew}).

2.2. Proposed modification of FAO-56

Eq. (7) reflects irrigation applied to the soil surface and infiltrating through the surface layer, as illustrated in Fig. 1A (from Allen et al., 1998). Under subsurface drip irrigation (SDI), irrigation water does not infiltrate (I_i) through the soil surface, but is applied at a specified depth in the soil and, consequently, moves in all directions depending upon the soil hydraulic properties (Fig. 1B). Therefore, only a fraction of the irrigation depth (I_i) travels towards the evaporation zone (defined as the top 0.10 to 0.15 m soil depth in Allen et al., 1998) due to capillary action, which depends on the soil type, soil heterogeneity, the initial water content, the hydraulic gradient acting on the soil surface, irrigation depths, root water uptake, the dripper discharge rate, and a burial depth of the drip line. Hence, there is a need to define the fraction of the irrigation depth that is exposed to evaporation ($f_{i,ES}$) under SDI. Incorporating

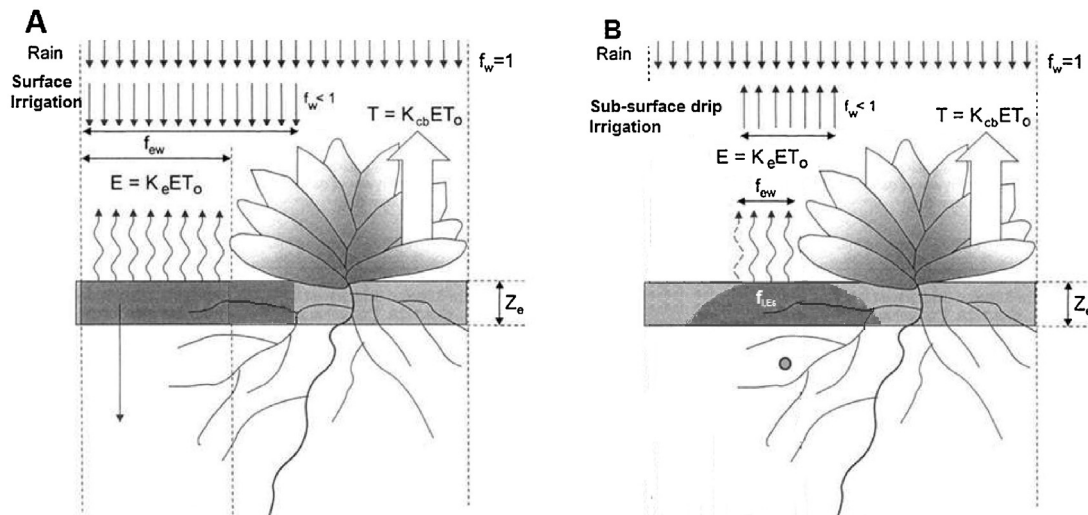


Fig. 1. Water balance of soil surface layer, as presented in FAO-56 (Eq.(7)) (from Allen et al., 1998) (A), and modified for SDI (Eq. (8)) (B).

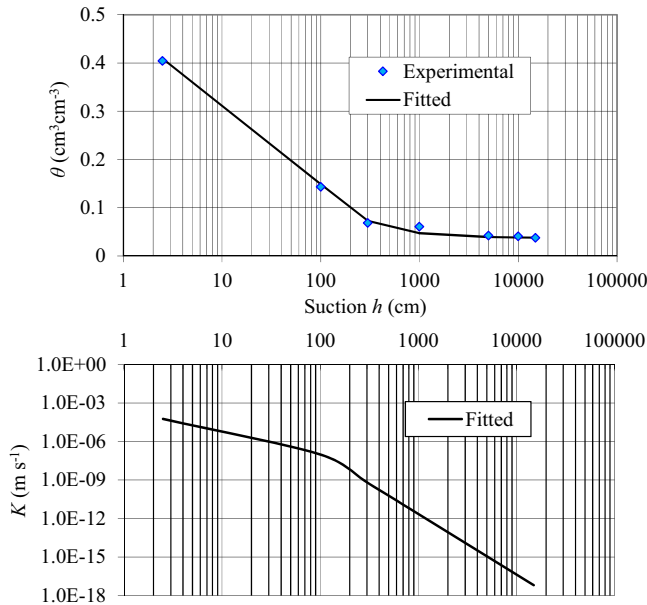


Fig. 2. Measured and fitted (van Genuchten, 1980) relationships between volumetric water content (θ) and pressure head (h); and a predicted relationship between hydraulic conductivity (K) and pressure head (h) for the 0–15 cm soil layer.

this consideration into FAO-56, Eq. (7) can be modified for SDI as follows:

$$D_{e,i} = D_{e,i-1} - (P_i - RO_i) - \frac{I_i \times f_{I,Es}}{f_w} + \frac{E_i}{f_{ew}} + T_{ew,i} + DP_{e,i} \quad (8)$$

where I_i is the applied irrigation depth (mm) and $f_{I,Es}$ represents the fraction of the irrigation depth that moves to the evaporation zone. Hence, $f_{I,Es}$ represents the fraction of the irrigation depth that is exposed to evaporation in the evaporation zone, and is 1 for all above ground irrigation systems, but ranges from 0 to 1 for SDI. This fraction will also impact the fraction of the soil surface wetted by irrigation (f_w), and therefore the fraction exposed and wetted (f_{ew}). All of the above fractions are depicted in Fig. 1B.

SDI impacts evaporation as described in Eq. (8) in two ways, at the irrigation input term (I_i/f_w) and at the evaporation term (E_i/f_{ew}). The impact on the irrigation input term is in the proportional refilling of the evaporation zone by irrigation, and thus a fractional term ($f_{I,Es}$) has been introduced to account for this, in addition to the

impact of SDI on f_w . In terms of the evaporation term, the only impact of SDI is on f_{ew} , which is derived from f_w . Consequently there is no need to modify the evaporation term of Eq. (8), rather just to account for the impact of SDI on f_w , and therefore on f_{ew} . However, it should be noted that f_w is assumed to be equal to 1 for rainfall (Allen et al., 1998).

Allen et al. (2005a,b) proposed an extension of evaporation estimation involving separate prediction of contribution from precipitation and from the wetted and exposed fraction. In such case the proposed modification for SDI conditions would be associated with the irrigation term only. The modified equation for the extended procedure would be similar to the above equation (Eq. (8)), while all other variables would remain similar to those explained in Allen et al. (2005a,b). However, for the comparison of the existing and modified procedures for the estimation of ET components, we use an earlier version (Allen et al., 1998) due to its wider acceptability even under partially wetting irrigation conditions (Flumignan et al., 2011; Fandiño et al., 2012; Paço et al., 2012; Martins et al., 2013; Cancela et al., 2015).

2.3. Estimation of the $f_{I,Es}$ and f_w fractions for the field site

In this investigation HYDRUS-2D was employed to compute the potential $f_{I,Es}$ and f_w for SDI in a vertical spatial domain of 335×100 cm. This domain was adopted based on the vine spacing in a field experiment conducted with Chardonnay wine grapes under subsurface drip (SDI) in the Markaranka vineyard (34.08°S and 139.87°E), located near Waikerie in South Australia. More details about the experimental layout, irrigation design, and water applications are given in Section 2.5 below and in Phogat et al. (2016, under review), in which the HYDRUS-2D model was calibrated and validated for two consecutive wine grape seasons. The same soil hydraulic and drip design parameters as in the field experiment are used in this study to compute f_w and $f_{I,Es}$ for SDI.

The soil hydraulic parameters for the experimental site were estimated from measured values of the water content-pressure head relationship. Water content-pressure head relations were measured using a tension plate (for pressure heads larger than -100 cm) and on a pressure plate (for pressures heads smaller than -100 cm down to $-15,000$ cm) apparatus on undisturbed soil core samples (Ford, 1997) taken at different depths (0–15, 15–30, 30–60 and 60–100 cm) at 4 locations within the trial site, and averaged between the 4 locations for each depth to represent the entire field site. The van Genuchten-Mualem constitutive relationship (van

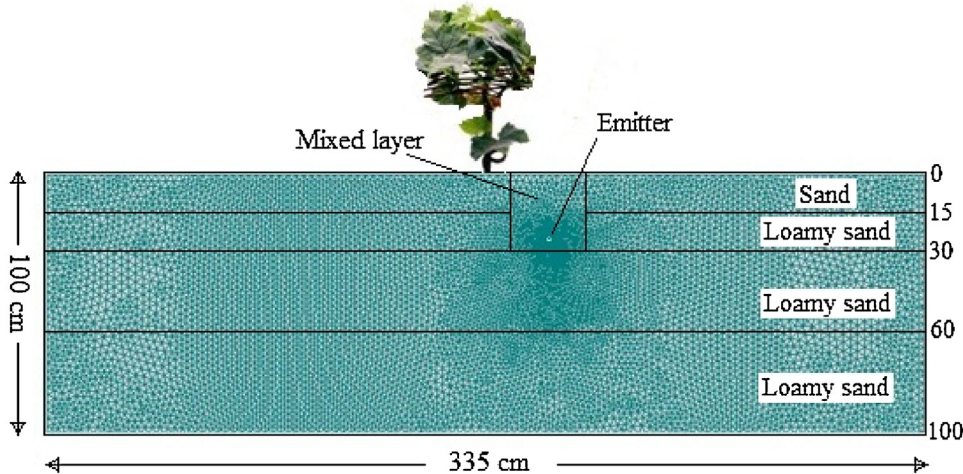


Fig. 3. Computational domain, spatial discretization and distribution of different soil horizons used for HYDRUS-2D simulation of the field site.

Genuchten, 1980) was fitted to measured soil water retention data and used to predict the unsaturated hydraulic conductivity function. Resulting θ - h and K - h relationships are depicted in Fig. 2 for the 0–15 cm soil depth.

The saturated hydraulic conductivity (K_s) and bulk density were also measured on the undisturbed soil cores following standard procedures (Klute, 1986). Estimated values of soil hydraulic parameters for different depths at the field site are given in Table 1 and were utilized as input parameters in HYDRUS-2D. Trenching or ripping activities associated with installation of SDI induce mixing of the soil directly above the drip line. Hence, average values of hydraulic parameters of the two upper layers (0–15 cm and 15–30 cm) were considered for that region (30 cm \times 30 cm) to represent the field conditions. The computational domain and its spatial discretization, as well as the distribution of soil horizons at the field site are shown in Fig. 3. Although the soil type description for all layers below the depth of 15 cm is the same (loamy sand), different hydraulic parameters were estimated based on laboratory measurements on undisturbed core samples. More details on parameterization, initial and boundary conditions, calibration and validation of HYDRUS-2D are given in Phogat et al. (2016 under review).

The transport domain was divided into two regions for mass balance calculations, the first region representing the evaporation zone extended from the soil surface to 15 cm (0–15 cm) soil depth, and the second region representing the remainder of the rootzone extended from 15 cm to 100 cm soil depth. The initial water content varied, based on measurements taken at the field site using calibrated Theta probes, from $0.05 \text{ cm}^3 \text{ cm}^{-3}$ at the soil surface to $0.17 \text{ cm}^3 \text{ cm}^{-3}$ at the bottom of the profile. These water contents match with the measured values from the soil cores. Since the goal of simulations was to assess the internal distribution of irrigation water within the two soil regions, a single irrigation application of 5 mm (approximately equal to the average amount of irrigation in the field experiment) was simulated, and the volume of water entering the evaporation zone was observed 24 h after the irrigation. Irrigation lasted for 4.1875 h, and the remaining time allowed for redistribution of the water applied. A similar procedure was adopted by Skaggs et al. (2004) and Kandalous and Šimůnek (2010) to examine the wetting front pattern under SDI in sandy loam and clay loam soils, respectively.

The irrigation system design is described in Section 2.5 below and in Phogat et al. (2016 under review). The difference between the initial and final volumes of water (after 24 h) in the first region (0–15 cm) is the amount of irrigation water that entered into the

evaporation zone, which was then expressed as a fraction of the water applied. Hence, $f_{i,Es}$ was estimated as the potential contribution of a single irrigation to the evaporation zone (0–15 cm soil depth). The simulated spatial extent of changes in water content (wetted length) was observed at the same time at the soil surface. The wetted length decreased from the bottom (at the 15 cm depth) to the top (at the soil surface, 0 cm) of the evaporation zone in a semi-circular fashion. Thus, the potential fraction of the soil surface wetted by irrigation (f_w) was estimated by dividing the wetted length with the distance between drip lines (or plant row spacing). Field measurements of Skaggs et al. (2004) indicate that closely placed drippers (30–40 cm) produce a continuously wetted soil surface of a uniform width above the drip tape. However, an exact surface area wetted by individual drippers may need to be estimated in other situations.

2.4. Impact of soil texture, soil heterogeneity, irrigation depth, and drip design parameters on the f_w and $f_{i,Es}$ fractions

Using the same computational domain and drip design parameters (drip line depth, emitter discharge, and spacing) as used for experimental conditions, the potential f_w and $f_{i,Es}$ fractions were estimated in the same way as described above for different uniform soil textures by changing the soil hydraulic parameters in the domain. Similarly, the impact of soil heterogeneity was evaluated by changing the soil hydraulic properties and layering within the domain. We evaluated the impact of two (Duplex) and three (Triplex) distinct layers of varied textures in the soil profile. A soil containing two distinct horizons of contrasting textures is known as a Duplex soil (Chittleborough, 1992). In the simulation, a loamy or sandy topsoil (0–30 cm) abruptly overlying much heavier textured subsoil (30–100 cm) was modelled. Such soils represent between half and two-thirds of the agricultural land in Australia (Tennant et al., 1992). Similarly Triplex soils show 3 distinct soil textural layers (0–15, 15–30, 30–100 cm) in the soil profile. The hydraulic parameters for these uniform soils and different heterogeneous layers in Duplex and Triplex soils were adapted from the HYDRUS database and are shown in Table 1. These parameters have been used in many similar studies (e.g. Assouline, 2002; Cote et al., 2003; Gärdenäs et al., 2005; Lazarovitch et al., 2009; El-Nesr et al., 2014) evaluating water movement and solute transport problems for drip irrigation systems. Two combinations of Duplex (sandy loam-clay loam and sandy loam-clay, respectively, in 0–30 and 30–100 cm soil depths) and Triplex (loamy sand-sandy loam-clay loam and loamy sand-sandy loam-clay, respectively, in 0–15, 15–30 and 30–100 cm

Table 1

Soil hydraulic parameters for the van Genuchten-Mualem function (van Genuchten, 1980) and the bulk density for different soil layers in a) field site soil, b) uniform soils, and c) heterogeneous soils.

Depths (cm)	Soil texture	Soil hydraulic parameters					Bulk density (g cm ⁻³)
		θ_r (cm ³ cm ⁻³)	θ_s (cm ³ cm ⁻³)	α (cm ⁻¹)	n	K_s (cm d ⁻¹)	
a) Field site soil (measured)							
0–15	Sand	0.04	0.41	0.03	2.09	561.60	0.52
15–30	Loamy sand	0.04	0.39	0.03	2.29	216.00	0.56
30–60	Loamy sand	0.05	0.38	0.04	1.70	259.20	0.41
60–100	Loamy sand	0.05	0.37	0.04	1.62	172.80	0.38
b) Uniform soils (from literature)							
0–100	Loamy sand	0.057	0.41	0.124	2.28	350.2	0.5
0–100	Loam	0.078	0.43	0.036	1.56	24.96	0.5
0–100	Clay loam	0.095	0.41	0.019	1.31	6.24	0.5
c) Heterogeneous soils: i) Duplex (from literature)							
0–30	Sandy loam	0.065	0.41	0.075	1.89	106.1	0.5
30–100	Clay loam	0.095	0.41	0.019	1.31	6.24	0.5
Heterogeneous soils: ii) Triplex (from literature)							
0–15	Loamy sand	0.057	0.41	0.124	2.28	350.2	0.5
15–30	Sandy loam	0.065	0.41	0.075	1.89	106.1	0.5
30–100	Clay	0.068	0.38	0.008	1.09	4.8	0.5

soil depths) were studied. Initial water contents were assumed to vary between air dry at the soil surface and field capacity at the bottom of the domain in all these simulations.

The impact of different irrigation depths (5, 7.5, 10, 12.5 and 15 cm) and SDI design parameters, i.e., different discharge rates (1.6, 2, 2.5, 3 and 4 L h⁻¹), different drip line depths (0, 10, 15, 20, 25 cm soil depth), and drip line spacings (100, 200 and 300 cm), on the evaporation fraction ($f_{i,Es}$) and the wetted fraction (f_w) was also evaluated in different uniform soil textures in the same vertical spatial domain shown in Fig. 3, by changing the corresponding irrigation depth, discharge rate, and emitter placement. Soil hydraulic properties for uniform soil textures (loamy sand, loam and clay loam) are shown in Table 1. Initial water contents for these simulations were also assumed to vary between air dry at the soil surface and field capacity at the bottom of the domain.

2.5. Comparison of ET components estimated by the original and modified FAO-56 procedures

The original and modified FAO-56 procedures were used to estimate annual ET components for the experimental field site in the SDI irrigated Chardonnay wine grape vineyard at Markaranka (34.08°S and 139.87°E), based on 2010–11 and 2011–12 climate data. The vineyard was planted in November 2004 at a vine spacing of 2.5 m and row spacing of 3.35 m. The SDI drip lines were placed 25 cm deep and 25 cm away from the vine row. The irrigation system consisted of a pressure compensated drip system (Toro Drip-In® Rootguard®) with emitters at a spacing of 40 cm with a discharge rate of 1.6 L h⁻¹. The soils at the site are predominately light textured, ranging from sand to loamy sand, with the sand content varying from 84 to 91% and small fractions of clay (9–13%) and silt (0–3%). Weather data were collected at an automated weather station located at Qualco, 4 km from the experimental site. The climate is characterized as dry, with warm to hot summers and mild winters. Total rainfall during the two experimental periods from 22 September 2010 to 30 June 2011 and from 7 September 2011 to 30 June 2012 was 338 mm and 236 mm, respectively. Grass reference evapotranspiration (ET_0) estimated using the FAO Penman-Monteith equation (Allen et al., 1998) during 2010–11 and 2011–12 growing seasons was 904 mm and 1055 mm, respectively. Mild frost conditions occurred during the winter months.

Local soil and climate parameters used to estimate E_s , T_p and ET_C for wine grapes for two seasons following the FAO-56 DCC

approach are given in Table 2. Tabulated crop coefficients for the initial (K_{cbini}), mid (K_{cbmid}) and late (K_{cbend}) seasons for wine grapes (Table 2) were taken from Allen and Pereira (2009) for a mid-density vineyard ($F_{ceff} = 0.5$). However, K_{cbmid} and K_{cbend} were adjusted depending on the prevailing minimum relative humidity, average wind speed and plant height as described in Allen et al. (1998). The adjusted values are given in Table 2.

The soils and irrigation water had salinity below threshold levels, hence osmotic stress due to salinity was not considered. Total available water (TAW) was estimated from the type of soil in each horizon (Table 1) and rooting depth (Z_r) (Table 2). The initial water deficit was estimated from measured water content data from the different soil layers (0–15, 15–30, 30–60, 60–100 cm) of the root zone. The field capacity (θ_{fc}) values for different layers are given in Table 2. The residual water content (θ_r , Table 1) was assumed as moisture content at wilting point (θ_{wp}) for the calculation of TAW which is a common approximation (van Genuchten, 1980). The θ_{fc} – θ_{wp} for different layers falls within the range reported in FAO-56 (Allen et al., 1998) for these soils. The readily available water (RAW) in the Z_r was estimated as per the equation given in FAO-56 (Allen et al., 1998):

$$RAW = pTAW \quad (9)$$

where, p is the average fraction of TAW that can be depleted from the root zone before moisture stress. It was estimated daily following a numerical approximation (Allen et al., 1998) adjusting p for daily ET_C :

$$p = p_{Table22} + 0.04(5 - ET_C) \quad (10)$$

where, $p_{Table22}$ value (0.45) for wine grape was taken from Allen et al. (1998). The estimated values of p during 2010–11 and 2011–12 varied from 0.33–0.64 and 0.35–0.65, respectively.

The readily evaporable water (REW) was shown to vary from 8 to 9 mm for the field soils (Stevens et al., 2012). Evaporation takes place from the exposed and wetted soil surface (f_{ew} , Eqs. (4), (7) and (8)) in drip irrigation systems, where only a fraction of the soil surface is wetted by irrigation application. Nonetheless, for orchards (e.g., wine grape) where f_w is exposed to large evaporative energy (Bonachela et al., 2001) and significant ventilation (Allen et al., 2005a), $f_{ew} = f_w$. However, for rainfall the effective surface exposed to evaporation (f_{ew}) is set equal 1– f_c (Allen et al., 2005a), where, f_c is the fraction of the soil surface shaded by the crop. Therefore, the

Table 2

Values of different parameters used to estimate daily transpiration (T_p) and daily evaporation (E_s) for wine grape for the field site following the original and modified FAO-56 DCC approaches.

Parameter	Value	Parameter	Value
$L_{ini}^{a,c}$	15	Plant height h (m) ^c	1.5
$L_{dev}^{a,c}$	30	Rooting depth Z_r (m) ^{a,c}	1.0
$L_{mid}^{a,c}$	100	Vineyard density (F_{ceff}) ^{a,c}	0.5
$L_{late}^{a,c}$	90	Evaporable depth Z_e (m) ^{a,d}	0.15
θ_{fc} (0–15 cm) ^c	0.09	Mid-season Min RH (%) (2010–11) ^c	27.0
θ_{fc} (15–30 cm) ^c	0.10	Mid-season Min RH (%) (2011–12) ^{a,c}	23.0
θ_{fc} (30–60 cm) ^c	0.11	Av. Wind speed (m/s) (2010–11) ^c	3.65
θ_{fc} (60–100 cm) ^c	0.12	Av. Wind speed (m/s) (2011–12) ^{a,c}	3.88
f_w , SDI ^e	0.22	K_{cb} ini ^d	0.20
f_w , Rain ^c	1	K_{cbmid} ^d	0.65
$f_{l,Es}^{b,e}$	0.42	K_{cbend} ^d	0.5
RAW (mm) ^c	34	$K_{cb midadj}$ (2010–11) ^c	0.76
TAW (mm) ^c	60	$K_{cb midadj}$ (2011–12) ^{a,c}	0.78
TEW (mm) ^c	12	$K_{cb endadj}$ (2010–11) ^c	0.61
REW (mm) ^c	8	$K_{cb endadj}$ (2011–12) ^{a,c}	0.63

^a Also used in uniform soils (loamy sand, loam and clay loam).

^b Used only in the modified FAO-56 approach.

^c Measured or estimated at field site.

^d Taken from literature.

^e Simulated using Hydrus-2D.

daily f_{ew} fraction during the crop season was estimated depending on the irrigation or rainfall event as outlined in Allen et al. (1998):

$$f_{ew} = \min(1 - f_c, f_w) \quad (11)$$

where, f_c is the fraction of the soil surface shaded by the crop. The variation of f_c during the vine growth was observed to vary from 0.01 to 50%. The maximum fraction of ground cover was attained during the mid-season of vine growth. The experimental area was kept weed free by adopting proper weed control operations during the experimental period, to minimise water losses through unwanted vegetation growth.

The values of f_w and $f_{l,Es}$ fractions (Table 2) were estimated numerically for field conditions described in Section 2.3. However, values of these (f_w and $f_{l,Es}$) and other empirical fractions and variables commonly used in FAO-56 may differ under cropped conditions. These values (f_w and $f_{l,Es}$) and other parameters shown in Table 2 were used to estimate E_s , T_p and ET_C for wine grapes under field conditions for two seasons using the original and modified procedures. In the original FAO-56 procedure the parameters shown in Table 2 were used except for the $f_{l,Es}$ fraction.

A similar comparison between the original and modified procedures for wine grape ET components (E_s , T_p and ET_C) was also made for theoretical uniform soils (loamy sand, loam, clay loam; Table 1) in order to understand the impact of soil texture on simulated results due to incorporation of the fraction of irrigation depth moving to the evaporation zone ($f_{l,Es}$) into the FAO-56 procedure. The values of various soil parameters and various fractions used in this estimation in different soils are shown in Table 3. Crop related and climate related data (marked in parenthesis of Table 2) were taken from the field condition dataset for 2011–12 season (Table 2). Total available water (TAW) in the top 1 m of the soil profile in loamy sand, loam and clay loam soils was estimated to be 40, 120 and 190 mm, respectively (Table 3). The REW and TEW values for these theoretical soils were taken from Allen et al. (1998). The values of the f_w and $f_{l,Es}$ fractions estimated in the previous section for uniform textures (loamy sand, loam and clay loam) given in Table 3 were used in the modified procedure. However, for the estimation of ET components by the original procedure, all parameters were the same except for the $f_{l,Es}$ fraction (Table 3), which is not required in the original FAO 56 procedure.

Table 3

Values of different parameters used to estimate daily transpiration (T_p) and daily evaporation (E_s) for wine grape in hypothetical uniform soils (loamy sand, loam and clay loam) following the original and modified FAO-56 DCC approaches.

Parameters	Values		
	Loamy sand	Loam	Clay loam
θ_{fc}^{c}	0.1	0.20	0.28
θ_{wp}^{c}	0.06	0.08	0.09
f_w , SDI ^d	0.03	0.07	0.09
f_w , Rain ^b	1	1	1
$f_{l,Es}^{a,d}$	0.05	0.16	0.17
TAW (mm) ^c	40	120	190
RAW (mm) ^c	25.5	73.4	116.2
TEW (mm) ^c	12	19	24
REW (mm) ^c	6	9	10

^a Used only in the modified FAO-56 approach.

^b Measured at field site.

^c Taken from literature.

^d Simulated using Hydrus-2D.

3. Results and discussion

3.1. Estimation of the $f_{l,Es}$ and f_w fractions for the field site

Results of HYDRUS-2D simulations of water movement under the field conditions and selected theoretical scenarios are presented in Table 4 and Fig. 4. In the field soil (s-ls-ls-ls), simulation results indicated that more than one-third of applied irrigation entered the evaporation zone ($f_{l,Es} = 0.42$), leading to a 0.22 wetted fraction (f_w) at the soil surface when the initial moisture content varied from air dry at the soil surface to field capacity at the bottom of the domain (top of Table 4, top right of Fig. 4). However, the $f_{l,Es}$ and f_w fractions varied greatly depending upon the initial moisture content in the soil (Table 4). The fraction of irrigation water entering the evaporation zone ($f_{l,Es}$) was reduced by a third under uniformly dry initial soil conditions (0.05–0.05), and increased slightly when initial soil conditions were wetter (0.08–0.20). Skaggs et al. (2010) also observed increased spatial spreading with higher antecedent water content after 24 h of simulation due to reduction in pores available to hold the applied water. Similarly, Provenzano (2007) also reported higher spatial distribution of applied water under SDI after a fixed time in response to greater initial moisture content. The initial water content had a similar impact on the fraction of the wetted surface (f_w).

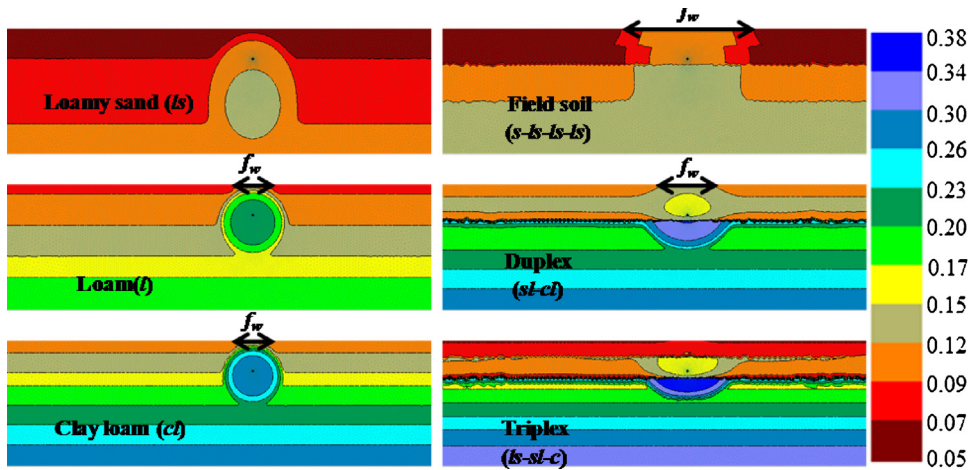


Fig. 4. Water content distribution and the wetted soil surface fraction (f_w) in different soils as simulated by HYDRUS-2D. The letters in parenthesis represent the textural class (s = sand, ls = loamy sand, sl = sandy loam, l = loam, cl = clay loam, c = clay) in the soil profile.

Table 4

Effect of soil texture, soil stratification, and initial water content on the evaporation fraction ($f_{i,Es}$) and the wetted surface fraction (f_w), as simulated using Hydrus 2D.

	Texture	Initial water content	$f_{i,Es}^e$	f_w^e
a) Field soils				
Sand-loamy sand	s-ls-ls-ls	0.05–0.17 ^a	0.42	0.22
Sand-loamy sand	s-ls-ls-ls	0.05–0.05 ^b	0.28	0.18
Sand-loamy sand	s-ls-ls-ls	0.08–0.20 ^c	0.44	0.30
b) Uniform soil texture				
Loamy sand	ls	0.06–0.10 ^d	0.05	0.03
Loam	l	0.08–0.20 ^d	0.16	0.07
Clay loam	cl	0.10–0.29 ^d	0.17	0.09
c) Soil heterogeneity				
Duplex	sl-cl	0.10–0.29 ^d	0.16	0.12
Duplex	sl-c	0.10–0.34 ^d	0.19	0.16
Triplex	ls-sl-cl	0.06–0.29 ^d	0.02	0.00
Triplex	ls-sl-c	0.06–0.34 ^d	0.01	0.00

^a Initial water content based on measured values.

^b Initial water content was low throughout the profile.

^c Initial water content varied from slightly wetter than air dry at the surface to higher than field capacity at the bottom of the profile.

^d Initial water content varied from air dry at the surface to field capacity at the bottom of the profile.

^e Simulated using Hydrus-2D.

3.2. Impact of soil texture and hydraulic properties on the $f_{i,Es}$ and f_w fractions

HYDRUS-2D simulations indicate that the $f_{i,Es}$ fraction in homogeneous and isotropic light textured (loamy sand) soil was minimal (0.04) for the same irrigation system parameters as used at the field site (Table 4). However, in medium- and heavy-textured soils $f_{i,Es}$ increased 4 times compared to light-textured soils. This implies that light textured soils are less prone to evaporation losses under SDI as compared to medium and heavy textured uniform soils. It is well known that capillary rise in medium- and heavy-textured soils is always higher than in light-textured soils due to their higher micro porosity. The fraction of the wetted surface (f_w) was higher in clay loam (0.09) than in loam soils (0.07) (Table 4 and Fig. 4).

HYDRUS simulations also indicated that soil heterogeneity had a pronounced impact on the fraction of irrigation water lost to evaporation. Amongst the duplex soils generally encountered in Australia, the sandy loam-clay combination had a higher surface wetness and evaporation fraction than other soil profiles (Table 4). When installed at a depth of 25 cm (as at the field site), the SDI was located in the light-textured soil just above the interface between the light and heavy-textured soils. In this profile, the heavy textured

soil acted as a physical barrier to downward water movement as the hydraulic gradient wasn't sufficient to overcome the boundary effect. Consequently the tendency of water movement towards the soil surface and laterally was increased, which led to a higher fraction of applied water reaching the evaporation zone. Similar observations were recorded by Finger (2012) for duplex soils with low permeability subsoils; the subsoil restricted downward movement, allowing water to spread laterally and upwards under subsurface irrigation.

Another modelled scenario (Triplex) involved a relatively coarse soil at the surface (0–15 cm) underlain by a finer soil (15–30 cm) (where the SDI was located), and a heavy soil below 30 cm. This scenario effectively reduced the evaporation fraction and restricted water movement to the soil surface because the soil interface at a depth of 15 cm acted as a barrier to water movement towards the surface. Hence, the presence of contrasting soil layers with different hydraulic parameters in the profile may act as a physical barrier and restrict water movement, and the location of the interfaces relative to the drip line depth can dramatically influence evaporation fluxes. These results suggest that a detailed soil analysis is important before designing subsurface drip systems, especially to determine the optimum installation depth (see below), so that undesirable water losses (E_s) can be minimized.

3.3. Impact of irrigation depth and drip design parameters on the $f_{i,Es}$ and f_w fractions

The impact of applying different irrigation depths (5, 7.5, 10, 12.5, and 15 cm) in different soil textures on the $f_{i,Es}$ and f_w fractions is shown in Fig. 5. While the $f_{i,Es}$ fraction gradually decreased with an increase in the irrigation depth in loamy sand, in loam it initially increased up to an irrigation depth of 10 cm and then decreased. In clay loam the $f_{i,Es}$ fraction increased with an increase in the irrigation depths, although the magnitude of the increase gradually decreased with larger irrigation depths. A larger extent of gravity compared to capillary forces in the coarse textured soils reduced the fraction of upward movement of applied irrigation water. On the other hand, the f_w fraction showed an increasing trend with an increase in irrigation depths in all soils. Average values of the f_w fraction were about 2.5 times higher in loam and clay loam than in loamy sand (Fig. 5), indicating a significant role of soil texture in evaporation losses from the soil.

The depth of the drip line placement in the soil had a pronounced impact on simulated evaporation fluxes and wetted surface fraction in different soils (Fig. 6). A drip line placed 10 cm deep in a

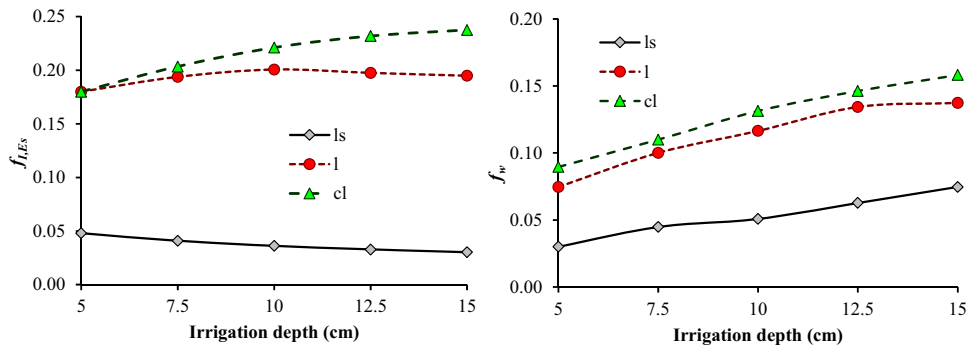


Fig. 5. Impact of irrigation depths on the fraction of irrigation contributing to evaporation ($f_{I,Es}$) and the fraction of the soil surface wetted by irrigation (f_w) in different soils (ls = loamy sand, l = loam, cl = clay loam) as simulated by HYDRUS-2D. The initial water content varied from dry at the surface to field capacity at the bottom in all simulations.

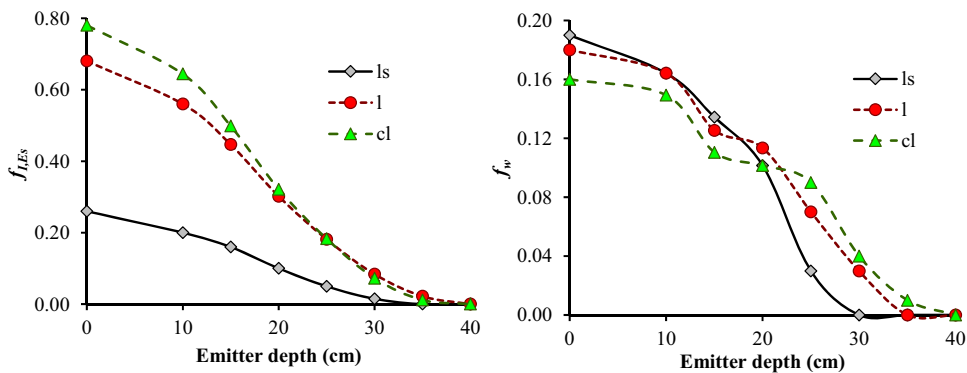


Fig. 6. Impact of the emitter depth on the fraction of irrigation contributing to evaporation ($f_{I,Es}$) and the fraction of the soil surface wetted by irrigation (f_w) in different soils (ls = loamy sand, l = loam, cl = clay loam) as simulated by HYDRUS-2D. The initial water content varied from dry at the surface to field capacity at the bottom in all simulations.

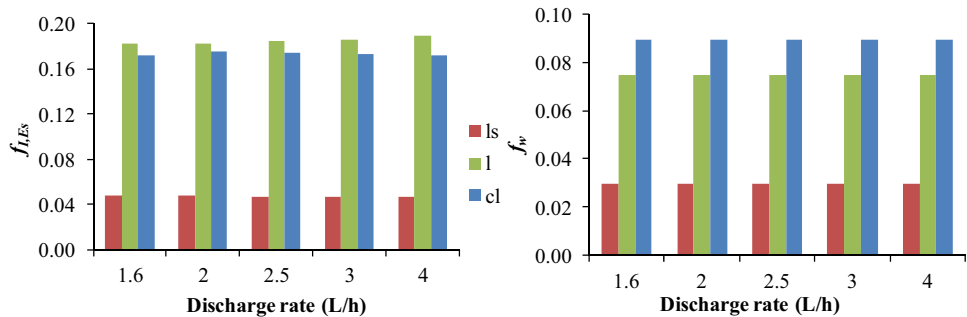


Fig. 7. Impact of the emitter discharge rate on the fraction of irrigation contributing to evaporation ($f_{I,Es}$) and the fraction of the soil surface wetted by irrigation (f_w) in different soils, as simulated by HYDRUS-2D (initial water content varied from dry at the surface to field capacity at the bottom in all simulations).

uniform soil had 25 to 64% of applied water available for evaporation depending on the soil texture, which was slightly lower than a dripline laid out at the soil surface (27–78%). Placing a drip line deeper than 10 cm gradually reduced the evaporation flux. The $f_{I,Es}$ fraction decreased by about two thirds for drip placed at a depth of 20 cm compared to drip on the soil surface in loamy sand, while this reduction was just over half in clay loam. Placing the drip 40 cm deep reduced the evaporation fraction to almost zero in uniform and isotropic soils. However, soil properties and soil heterogeneity play a key role in the spatial distribution of irrigation water. It is expected that drip placed at a depth of 40 cm is likely to increase water losses via deep percolation. Similar observations have been made in other studies as well (Evett et al., 1995; Diamantopoulos and Elmaloglou, 2012). Hence, a trade-off exists between reducing evaporation losses and increasing deep percolation losses under sub-surface drip irrigation. A similar effect of the drip placement on the wetted fraction (f_w) was observed (Fig. 6). However, the

extent of the reduction in the evaporation fraction ($f_{I,Es}$) was higher than the corresponding reduction in the wetted fraction (f_w) as the depth of the drip line placement increased (Fig. 6). On the other hand, applying the same quantity of water with different drip discharge rates showed little impact on $f_{I,Es}$ and f_w within a given soil type (Fig. 7), for example for loam soils (green bars) $f_{I,Es} = 0.18\text{--}0.19$, $f_w = 0.07$.

The drip line spacing strongly influenced the wetted fraction (f_w) of the soil surface (Fig. 8). When the drip line spacing was reduced by two thirds, the wetted fraction increased proportionally, as the total surface area for one drip line (a denominator in fraction calculations) was reduced. Hence, the surface drip with 100 cm spacing wetted about 60% of the soil surface, whereas f_w decreased to 20% when the drip spacing increased to 300 cm. This proportional relationship was roughly maintained as the dripline depth increased, until f_w approached zero for the 35 cm depth.

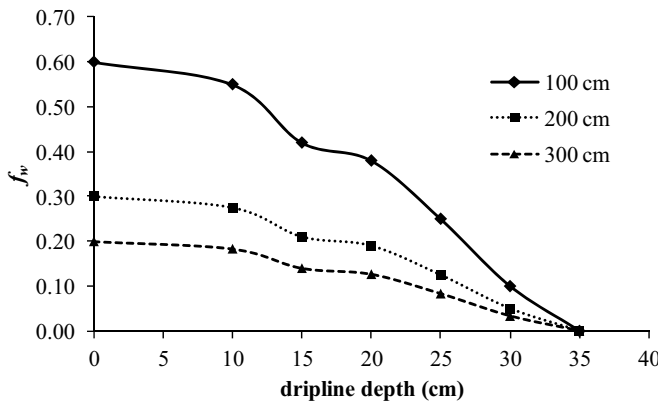


Fig. 8. Effect of the drip line spacing on the wetted surface fraction (f_w) for different emitter depths in a loam soil, as simulated by HYDRUS-2D (water content varied from dry at the surface to field capacity at the bottom in all simulations).

A strong correlation ($R^2 = 0.92$) was observed between $f_{I,Es}$ and f_w as a function of soil properties (data from Table 1) whereas the correlation was moderately good ($R^2 = 0.66$) for drip design parameters (data from Figs. 6 and 7), as shown in Fig. 9. These results reinforce the conclusion made above that a comprehensive analysis of soil and drip design parameters is important before drip systems are installed, in order to minimise irrigation losses due to evaporation.

3.4. Comparison of the modified approach with FAO-56 for estimating seasonal evaporation

The modified FAO-56 procedure incorporating the $f_{I,Es}$ fractions according to Eq. (8) was compared with the existing FAO-56 approach for estimating annual ET components for a grapevine irrigated with SDI. Annual evaporation (E_s) estimated using the standard FAO-56 procedure was 208.7 mm and 184.2 mm during the 2010–11 and 2011–12 seasons, respectively (Table 5). However, annual E_s values estimated with the modified procedure amounted to 197.9 mm and 173.3 mm during the 2010–11 and 2011–12 seasons, respectively. Average annual evaporation was thus slightly overestimated (5–6%) using the standard FAO-56 procedure compared to using the modified procedure. However, this deviation in seasonal evaporation can increase further depending on the soil texture. Predicted scenarios in uniform soils showed that the difference in seasonal E_s between the original and modified FAO-56 procedures varied between 7 and 18% when soil texture increased from loamy sand to clay loam (Table 5). Overestimation of the evaporation flux had a depressing impact on the transpiration flux

estimated by the DCC approach (up to 4%). This impact would ultimately transmit to the estimation of basal crop coefficients, net irrigation and irrigation scheduling, and could affect the growth and yield of the crop.

Based on the results reported above it is recommended that the impact of sub-surface irrigation on the movement of water into the evaporation zone be incorporated into the existing FAO-56 procedure to improve estimates of ET components for crops under SDI. We have described and demonstrated a potential method for incorporating this component, using the fraction of irrigation water contributing towards evaporation losses ($f_{I,Es}$). However, the values of these fractions can vary in more complex and highly dynamic cropped conditions.

4. Conclusions

Optimization of irrigation is necessary for managing scarce water resources and for enhancing the water productivity and efficiency of irrigated systems. This requires a reduction in undesirable losses of water due to evaporation, especially under controlled irrigation with subsurface drip. Evaporation under SDI can be effectively estimated if an accurate evaluation of the fraction of irrigation water entering the evaporation zone can be made. This study estimated potential values of this fraction for different soils, irrigation depths and drip design parameters and integrated this into the FAO-56 DCC approach for the estimation of evaporation and ET partitioning for SDI of wine grapes. This method can further improve our understanding of evaporation losses under highly water efficient irrigation systems, particularly in sparsely vegetated crops.

As an improvement to the existing FAO-56 procedure, which assumes that all irrigation water contributes to evaporation losses, we have proposed to incorporate into the existing DCC procedure a variable which defines the fraction of irrigation water contributing towards evaporation losses ($f_{I,Es}$). We have demonstrated how an understanding of the impact of soil texture, soil heterogeneity, irrigation depth, and design parameters of an irrigation system on $f_{I,Es}$ can help in developing an appropriate irrigation system design according to soil parameters at the site, consequently reducing evaporation under field conditions. Annual estimation of evaporation and transpiration fluxes under SDI of wine grapes showed considerable variation in these fluxes. The overestimation of annual evaporation using the existing FAO-56 DCC approach ranged from 5 to 6% under conditions at the field site over two seasons. However, this over-estimation was shown to increase further (up to 18%) for different soil textures, and may vary under other crop and climatic conditions. Understanding these variations can be helpful when devising efficient irrigation scheduling for crops under SDI, and can assist in reducing undesirable water losses through evapo-

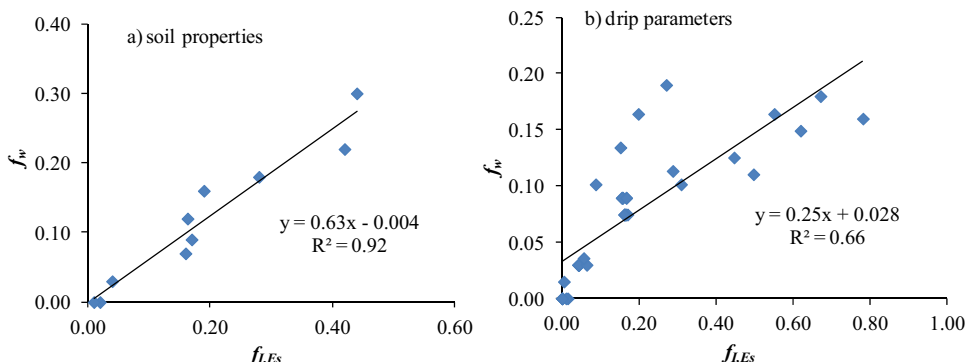


Fig. 9. Relationship between the fraction of the surface wetted (f_w) and the fraction of the irrigation contribution to evaporation ($f_{I,Es}$) as influenced by a) soil characteristics and b) drip design parameters, simulated by HYDRUS-2D.

Table 5

Impact of the wetted (f_w) and evaporation ($f_{I,Es}$) fractions on the seasonal ET components for SDI-irrigated wine grape, estimated by the original FAO-56 procedure and the modified approach for two seasons in field soil, and predicted scenarios for uniform soils using 2011–12 field data.

Soil type	Wetted fraction (f_w) ^a	Evaporation fraction ($f_{I,Es}$) ^a	E_s (mm)	ET_C (mm)	T_p (mm)
Field soil (2010–11)					
Original FAO 56	0.22	–	208.7	587.1	378.4
Modified FAO-56	0.22	0.42	197.9	584.3	386.4
Over-estimation (%)			5.5	0.5	–2.1
Field soil (2011–12)					
Original FAO-56	0.22	–	184.2	532.8	348.6
Modified FAO-56	0.22	0.42	173.3	530.4	357.0
Over-estimation (%)			6.3	0.5	–2.4
Uniform loamy sand soil (2011–12)					
Original FAO-56	0.03	–	99.6	472.8	373.2
Modified FAO-56	0.03	0.05	93.0	471.8	378.8
Over-estimation (%)			7.2	0.2	–1.5
Uniform loam soil (2011–12)					
Original FAO-56	0.07	–	138.3	582.0	443.6
Modified FAO-56	0.07	0.16	125.9	578.7	452.8
Over-estimation (%)			9.8	0.6	–2.0
Uniform clay loam soil (2011–12)					
Original FAO-56	0.09	–	159.5	647.1	487.6
Modified FAO-56	0.09	0.17	135.0	641.4	506.4
Over-estimation (%)			18.2	0.9	–3.7

^a Simulated using Hydrus-2D.

ration. We believe that a procedural change in the estimation of E_s for the FAO-56 approach would help in improving the estimation of evaporation and transpiration under sparsely vegetated and SDI-irrigated soil conditions, and that this information can be utilized when developing better irrigation management practices for crops under SDI. However, there is still a need to evaluate the impact of the proposed modification on the evaporation losses under different crops, soils, and climatic conditions.

Acknowledgements

The work was conducted by the South Australian Research and Development Institute, a member of the Wine Innovation Cluster at the Waite Precinct in Adelaide, and is supported by Australian grape growers and winemakers through their investment body, the Grape and Wine Research and Development Corporation, with matching funds from the Australian Government. We would also like to acknowledge the support of Treasury Wine Estates and their staff at the Markaranka vineyard for facilitating site access and support, and for installing the SDI trial used for this project. We thank the editors and anonymous reviewers for their constructive inputs during the review phase of the paper.

References

- Šimůnek, J., van Genuchten, M.Th., Šejna, M., 2008. Development and applications of the HYDRUS and STANMOD software packages and related codes. Vadose Zone J. 7 (2), 587–600, <http://dx.doi.org/10.2136/VZJ2007.0077>.
- Šimůnek, J., van Genuchten, M.Th., Šejna, M., 2016. Recent developments and applications of the HYDRUS computer software packages. Vadose Zone J. 15 (7), 25, <http://dx.doi.org/10.2136/vzj2016.04.0033>.
- Allen, R.G., Pereira, L.S., 2009. Estimating crop coefficients from fraction of ground cover and height. Irrig. Sci. 28, 17–34.
- Allen, R.G., Pereira, L.S., Raes, D., Smith, M., 1998. Crop Evapotranspiration: Guidelines for Computing Crop Water Requirements FAO Irrigation and Drainage Paper No. 56. FAO, Rome, Italy.
- Allen, R.G., Pereira, L.S., Smith, M., Raes, D., Wright, J.L., 2005a. FAO-56 dual crop coefficient method for estimating evaporation from soil and application extensions. J. Irrig. Drain. Eng. 131, 2–13.
- Allen, R.G., Pruitt, W.O., Raes, D., Smith, M., Pereira, L.S., 2005b. Estimating evaporation from bare soil and the crop coefficient for the initial period using common soil information. J. Irrig. Drain. Eng. 131, 14–23.
- Allen, R.G., 2000. Using the FAO-56 dual crop coefficient method over an irrigated region as part of an evapotranspiration inter-comparison study. J. Hydrol. 229 (1–2), 27–41.
- Assolouine, S., 2002. The Effects of microdrip and conventional drip irrigation on water distribution and uptake. Soil Sci. Soc. Am. J. 66, 1630–1636.
- Bonachela, S., Orgaz, F.O., Villalobos, F.J., Fereres, E., 2001. Soil evaporation from drip-irrigated olive orchards. Irrig. Sci. 20, 65–71.
- Burt, C.M., Muztiger, A.J., Allen, R.G., Howell, T.A., 2005. Evaporation research: review and interpretation. J. Irrig. Drain. Eng. 131 (1), 37–58.
- Cancela, J.J., Fandiño, M., Rey, B.J., Martínez, E.M., 2015. Automatic system based on dual crop coefficient, soil and plant water status for *Vitis Vinifera* (cv Godello and Mencía). Agric. Water Manage. 151, 52–63.
- Chanzly, A., Bruckler, L., 1993. Significance of soil surface moisture with respect to daily bare soil evaporation. Water Resour. Res. 29, 1113–1125.
- Chittleborough, D.J., 1992. Formation and pedology of duplex soils. Aust. J. Exp. Agric. 32, 815–825.
- Cote, C.M., Bristow, K.L., Charlesworth, P.B., Cook, F.J., Thorburn, P.J., 2003. Analysis of soil wetting and solute transport in subsurface trickle irrigation. Irrig. Sci. 22, 143–156.
- Diamantopoulos, E., Elmaloglou, S., 2012. The effect of drip line of surface and subsurface drip irrigation. Irrig. Drain. 61, 622–630.
- El-Nesr, M.N.B., Alazba, A., Šimůnek, J., 2014. HYDRUS simulations of the effects of dual-drip subsurface irrigation and a physical barrier on water movement and solutes transport in soils. Irrig. Sci. 32 (2), 11–125.
- Elmaloglou, S., Soulis, K.X., Dercas, N., 2013. Simulation of soil water dynamics under surface drip irrigation from equidistant line sources. Water Resour. Manage. 27, 4131–4148.
- Evett, S.R., Howell, T.A., Schneider, A.D., 1995. Energy and water balances for surface and sub-surface drip irrigated corn. In: Proceedings of Fifth International Micro-irrigation Congress, April 2–6, Orlando, USA, pp. 135–140.
- Fandiño, M., Cancela, J.J., Rey, B.J., Martinez, E.M., Rosa, R.G., Pereira, L.S., 2012. Using the dual-Kc approach to model evapotranspiration of Albariño vineyards (*Vitis vinifera* L cv. Albariño) with consideration of active ground cover. Agric. Water Manage. 112, 75–87.
- Finger, L., 2012. Suitability of Subsurface Drip Irrigation for Sustainable Pasture Production in the Riverine Plain Ph.D. Thesis. Department of Agriculture and Food Systems and Department of Infrastructure Engineering, The University of Melbourne.
- Flumignan, D.L., Faria, R.T., Prete, C.E.C., 2011. Evapotranspiration components and dual crop coefficients of coffee trees during crop production. Agric. Water Manage. 98, 791–800.
- Ford, E.J., 1997. Soil Water Retention Determination Using the 'Wetlab' Facility at CSIRO, Davies Laboratory, Technical Report 2/97. CSIRO Land and Water, Australia, <http://www.clw.csiro.au/publications/technical97/tr2-97.pdf> (accessed 20.06.16.).
- Gärdénäs, A.I., Hopmans, J.W., Hanson, B.R., Šimůnek, J., 2005. Two-dimensional modeling of nitrate leaching for various fertilization scenarios under micro-irrigation. Agric. Water Manage. 74, 219–242.
- Kanelous, M.M., Šimůnek, J., 2010. Numerical simulations of water movement in a subsurface drip irrigation system under field and laboratory conditions using HYDRUS-2D. Agric. Water Manage. 97, 1070–1076.

- Kandelous, M.M., Kamai, T., Vrugt, J.A., Šimůnek, J., Hanson, B., Hopmans, J.W., 2012. Evaluation of subsurface drip irrigation design and management parameters for alfalfa. *Agric. Water Manage.* 109, 81–93.
- Klute, A., 1986. Methods of soil analysis, part 1, physical and mineralogical methods 2nd ed. American Society of Agronomy, Agronomy Monographs 9(1), Madison, Wisconsin.
- Kool, D., Agam, N., Lazarovitch, N., Heitman, J.L., Sauer, T.J., Ben-Gal, A., 2014a. A review of approaches for evapotranspiration partitioning. *Agric. For. Meteorol.* 184, 56–70.
- Kool, D., Ben-Gal, A., Agam, N., Šimůnek, J., Heitman, J.L., Sauer, T.J., Lazarovitch, N., 2014b. Spatial and diurnal below canopy evaporation in a desert vineyard: measurements and modelling. *Water Resour. Res.* 50, <http://dx.doi.org/10.1002/2014WR015409>.
- Lazarovitch, N., Šimůnek, J., Shani, U., 2005. System-dependent boundary condition for water flow from subsurface source. *Soil Sci. Soc. Am. J.* 69 (1), 46–50.
- Lazarovitch, N., Poulton, M., Furman, A., Warrick, A.W., 2009. Water distribution under trickle irrigation predicted using artificial neural networks. *J. Eng. Math.* 64, 207–218.
- Li, X., Shi, H., Šimůnek, J., Gong, X., Peng, Z., 2015. Investigation of soil water dynamics in a drip irrigated strip intercropping field under plastic mulch. *Irrig. Sci.* 33, 289–302.
- Martins, J.D., Rodrigues, G.C., Paredes, P., Carlesso, R., Oliveira, Z.B., Knies, A.E., Petry, M.T., Pereira, L.S., 2013. Dual crop coefficients for maize in southern Brazil: model testing for sprinkler and drip irrigation and mulched soil. *Biosyst. Eng.* 115 (3), 291–310.
- Naglic, B., Kechavarzi, C., Coulon, F., Pintar, M., 2014. Numerical investigation of the influence of texture, surface drip emitter discharge rate and initial soil moisture condition on wetting pattern size. *Irrig. Sci.* 32 (6), 421–436.
- Paço, T.A., Ferreira, M.I., Rosa, R.D., Paredes, P., Rodrigues, G.C., Conceicao, N., Pacheco, C.A., Pereira, L.S., 2012. The dual crop coefficient approach using a density factor to simulate the evapotranspiration of a peach orchard: SIMDualKc model versus eddy covariance measurements. *Irrig. Sci.* 30, 115–126.
- Phogat, V., Mahadevan, M., Skewes, M., Cox, J.W., 2012. Modeling soil water and salt dynamics under pulsed and continuous surface drip irrigation of almond and implications of system design. *Irrig. Sci.* 30 (4), 315–333.
- Phogat, V., Skewes, M.A., Mahadevan, M., Cox, J.W., 2013. Evaluation of soil plant system response to pulsed drip irrigation of an almond tree under sustained stress conditions. *Agric. Water Manage.* 118, 1–11.
- Phogat, V., Skewes, M., Cox, J.W., Sanderson, G., Alam, J., Šimůnek, J., 2014. Seasonal simulation of water, salinity, chloride and nitrate dynamics under drip irrigated mandarin (*Citrus reticulata*) and assessing management options for drainage and nitrate leaching. *J. Hydrol.* 513, 504–516.
- Phogat, V., Skewes, M., McCarthy, M.G., Cox, J.W., Šimůnek, J., Petrie, P.R., 2016. Evaluation of crop coefficients, water productivity, and water balance components for wine grapes irrigated at different deficit levels by a sub-surface drip. *Agric. Water Manage.* (under review).
- Provenzano, G., 2007. Using HYDRUS-2D simulation model to evaluate wetted soil volume in subsurface drip irrigation systems. *J. Irrig. Drain. Eng.* 133 (4), 342–349.
- Ramos, T.B., Šimůnek, J., Goncalves, M.C., Martins, J.C., Prazeres, A., Pereira, L.S., 2012. Two-dimensional modeling of water and nitrogen fate from sweet sorghum irrigated with fresh and blended saline waters. *Agric. Water Manage.* 111, 87–104.
- Ritchie, J.T., 1972. Model for predicting evaporation from a row crop with incomplete cover. *Water Resour. Res.* 8, 1204–1213.
- Singh, D.K., Rajput, T.B.S., Sikarwar, H.S., Sahoo, R.N., Ahmed, T., 2006. Simulation of soil wetting pattern with subsurface drip irrigation from line source. *Agric. Water Manage.* 83, 130–134.
- Skaggs, T.H., Trout, T.J., Šimůnek, J., Shouse, P.J., 2004. Comparison of HYDRUS-2D simulations of drip irrigation with experimental observations. *J. Irrig. Drain. Eng.* 130 (4), 304–310.
- Skaggs, T.H., Trout, T.J., Rothfuss, Y., 2010. Drip irrigation water distribution pattern: effects of emitter rate, pulsing and antecedent water. *Soil Sci. Soc. Am. J.* 74, 1886–1896.
- Stevens, R.M., Ewenz, C.M., Grigson, G., Conner, S.M., 2012. Water use by an irrigated almond orchard. *Irrig. Sci.* 30 (3), 189–200.
- Tennant, D., Scholtz, G., Dixon, J., Purdie, B., 1992. Physical and chemical characteristics of duplex soils and their distributions in the south-west of Western Australia. *Aust. J. Exp. Agric.* 32, 827–843.
- Torres, E.A., Calera, A., 2010. Bare soil evaporation under high evaporation demand: a proposed modification to the FAO-56 model. *Hydrol. Sci. J.* 55 (3), 303–315.
- van Genuchten, M.Th., 1980. A closed-form equation for predicting the hydraulic conductivity of unsaturated soils. *Soil Sci. Soc. Am. J.* 44, 892–898.